PASJ: Publ. Astron. Soc. Japan **48**, L59–L63 and Plate 18 (1996)

Detection of the Mid-Infrared Unidentified Bands in the Diffuse Galactic Emission by IRTS

Takashi ONAKA
Department of Astronomy, School of Science, The University of Tokyo, Bunkyo-ku, Tokyo 113
E-mail (TO): onaka@astron.s.u-tokyo.ac.jp

Issei YAMAMURA* and Toshihiko TANABÉ
Institute of Astronomy, Faculty of Science, The University of Tokyo, 2-21-1 Osawa, Mitaka, Tokyo 181
and
Thomas L. ROELLIG and Lunming YUEN†
NASA Ames Research Center, MS245-6, Moffett Field, CA 94035, U.S.A.

(Received 1996 July 3; accepted 1996 August 27)

Abstract

This letter presents the first results of the mid-infrared spectrum (4.5–11.7 μm) of the diffuse emission near to the galactic plane ($l \sim 50°$; $|b| \leq 5°$) obtained by the mid-infrared spectrometer on board the Infrared Telescope in Space mission. The results clearly demonstrate the presence of unidentified infrared emission (UIR) bands at 6.2, 7.7, 8.6, and 11.3 μm in the diffuse galactic emission. The distribution of the UIR bands correlates well with the IRAS 100 μm map, suggesting that the UIR-band emitting material is well mixed with the classical dust grains in general interstellar space. The present results indicate that more than 70% of the IRAS 12 μm flux diffuse emission is emitted in the spectral range 8–11.7 μm, and that most of the 12 μm excess comes from the features associated with the UIR bands.

Key words: Infrared: diffuse emission — Infrared: spectra — Interstellar: dust — Spacecraft

1. Introduction

The IRAS observations have shown that there is excess emission in the IRAS 12 μm band in the diffuse interstellar clouds, emission greater than that expected from the classical interstellar dust grains of submicron size that give rise to the far infrared emission (Boulanger et al. 1985). This excess has been interpreted in terms of very small dust grains with fluctuating temperature (Draine, Anderson 1985), or alternatively may be due to emission from the so-called unidentified infrared (UIR) emission bands, rather than a smooth continuum (Puget et al. 1985). The UIR bands are a family of emission bands which have been observed in various celestial objects, including planetary nebulae, reflection nebulae, and H II regions. The main components of the UIR bands are located at 3.3, 6.2, 7.7, 8.6, and 11.3 μm, and are generally thought to be of carbonaceous origin.

Observations by a balloon-borne experiment, AROME, have detected the 3.3 μm UIR emission band in the diffuse galactic emission, supporting the idea that the carriers are present in general interstellar space (Giard et al. 1988, 1989). Recently Ristorcelli et al. (1994) have also reported the detection of the 6.2 μm band in the diffuse galactic emission by the AROME experiment. The UIR bands at 7.7, 8.6, and 11.3 μm, which are in the IRAS 12 μm passband, and would therefore contribute to the IRAS 12 μm excess directly, have however not yet been measured in the diffuse galactic emission. The detection of the 3.3 and 6.2 μm UIR bands strengthens the significance of a spectroscopic study of diffuse emission in order to elucidate the nature of the 12 μm excess emission.

Various candidates have been proposed for the origin of the UIR bands. Among them are polycyclic aromatic hydrocarbons (PAH; Léger, Puget 1984; Allamandola et al. 1985), a quenched carbonaceous composite (QCC; Sakata et al. 1984, 1987), hydrogenated amorphous carbon (HAC; Duley, Williams 1981; Borghesi et al. 1987), and coal grains (Papoular et al. 1989). The relative spatial distributions of the UIR bands in various interstellar conditions, if they do exist in general interstellar space, should provide important information to identify the carrier as well as the emission mechanism of the UIR bands.

This letter presents the first results concerning the mid-IR spectrum (4.5–11.7 μm) of diffuse emission obtained by the Mid-IR Spectrometer (MIRS) on board

* Present address: SRON-Groningen, Landleven 12, P.O.Box 800, 9700 AV Groningen, The Netherlands.
† Present address: Astronomy Program, University of Massachusetts, Lederle Graduate Research Tower B538, Amherst, MA 01003, U.S.A.

the Infrared Telescope in Space (IRTS). The results provide the mid-IR spectrum of the diffuse emission around the galactic plane for the first time, and unambiguously demonstrate the presence of the 6.2, 7.7, 8.6, and 11.3 μm UIR bands. The 3.3 μm band in the diffuse galactic emission has been observed by the Near-IR Spectrometer (NIRS) on board the IRTS, and is reported separately (Tanaka et al. 1996).

2. Observations and Data Reduction

The design and flight operations of the IRTS mission have been described by Murakami et al. (1994, 1996). This letter reports on an analysis of the data around the galactic plane ($|b| \leq 5°$ and $44° \leq l \leq 54°$), where accurate pointing information is presently available. The MIRS is a low-resolution spectrometer with a field of view of $8' \times 8'$, and covers the spectral range of 4.5–11.7 μm with 32 discrete detectors. The spectral resolution is approximately 0.3 μm and has been optimized for the spectroscopic study of extended objects. Details concerning the MIRS design and expected performance are given in Roellig et al. (1994).

Concerning the results reported here, the sensitivity of shorter wavelength channels of the MIRS (≤ 6 μm) has been calibrated based upon the standard stars observed on orbit whose calibrated spectra have been provided by a systematic investigation of infrared calibration sources for space missions (Cohen et al. 1995). A calibrated spectrum of Ceres, taken at about the same time as the MIRS observations (Cohen, private communication), was used for calibrating the longer MIRS wavelength channels (≥ 6 μm). Details concerning the signal processing of point sources are described in Yamamura et al. (1996). The flight-beam pattern has also been determined based on the observed profile of point sources. Including the errors in the absolute calibration, based on the standard objects and those in the beam-pattern, we estimate that the current absolute accuracy of the MIRS for diffuse emission is approximately 30%. The error comes mostly from the beam-pattern correction. Although the beam pattern shows a gradual dependence on the wavelength (20% between both ends of the spectral range), the spectral features within a narrow wavelength range are not affected by the correction. The wavelength calibration is based on a pre-flight measurement. The estimate of the UIR band strengths should not be affected by minor changes in the wavelength calibration.

The data were rearranged into $4' \times 4'$ grids in the region observed in $44° \leq l \leq 54°$ and $|b| \leq 5°$. We used the time-differentiated signal at each sampling point to maximize the spatial resolution. An improvement of the signal-to-noise ratio is expected in future data processing if the integration amplifier advantage is fully employed (Roellig et al. 1994).

The zodiacal emission dominates the background emission in the observed spectral range. In order to extract the galactic diffuse emission as well as to reduce any spurious features which may arise from the possible residual dark current, we define the background emission level outside of the galactic plane and subtract it from the data. Since the IRTS mission did not cover the whole sky, we cannot define a baseline for constant ecliptic longitudes. Instead, we averaged the observed emission around $\beta = 28°$ and 44° near to $l \sim 50°$, outside of the target area shown in figure 2 (Plate 18), and drew a straight line between these points as an estimate of the combined zodiacal emission background and dark current for each spectral channel. The galactic plane is located around $30° \leq \beta \leq 42°$ at this galactic longitude. Although this procedure may overestimate the zodiacal emission by 5×10^{-8} W m^{-2}sr^{-1} at most, it provides a reasonable baseline for the following analysis. It does not introduce any serious errors in the estimate of the band strengths.

3. Results and Discussion

The spectra obtained as described in the previous section are shown in figure 1. The galactic-plane spectrum (solid line) is from a region located at $44° \leq l \leq 44°44'$ and $-0°40' \leq b \leq 0°$, which was selected to exclude bright spots, and to sample only the diffuse emission. The spectra taken in the $50° \leq l \leq 53°$ and $1° \leq b < 2°$, $50° \leq l \leq 53°$ and $2° \leq b < 3°$, and $51° \leq l \leq 54°$ and $3° \leq b \leq 5°$ regions are also plotted by a dashed line, a dotted line, and a dot-dashed line, respectively. These clearly show the presence of the 6.2, 7.7, 8.6, and 11.3 μm UIR bands and the decrease in their strengths with the galactic latitude. The "plateau" between 5.5 and 9 μm is also seen in the spectra.

The weak components of the UIR bands, such as the 5.2, 5.6, and 6.9 μm bands, which have been claimed to belong to the UIR family (Bregman et al. 1983; Cohen et al. 1986; Allamandola et al. 1989), are not clearly seen in the present spectra. Further analysis is needed to confirm a possible excess at around 5.2 μm. An upper limit of these bands in the galactic plane region is approximately 2×10^{-8} W m^{-2} sr^{-1}. The 5.6 and 6.9 μm bands have not been detected in all of the objects with the major UIR band components (Cohen et al. 1989). The possible absence of weak bands in the galactic diffuse emission may provide a clue to identify the UIR band carrier in interstellar space.

In order to estimate the UIR band strength quantitatively we need to define the continuum level. For our data analysis, we drew a straight line between the edges of the feature for each band, and extracted the flux above the lines as the band strength. The wavelength points defined for the straight continuum are 5.95 and 6.64 μm, 7.09 and

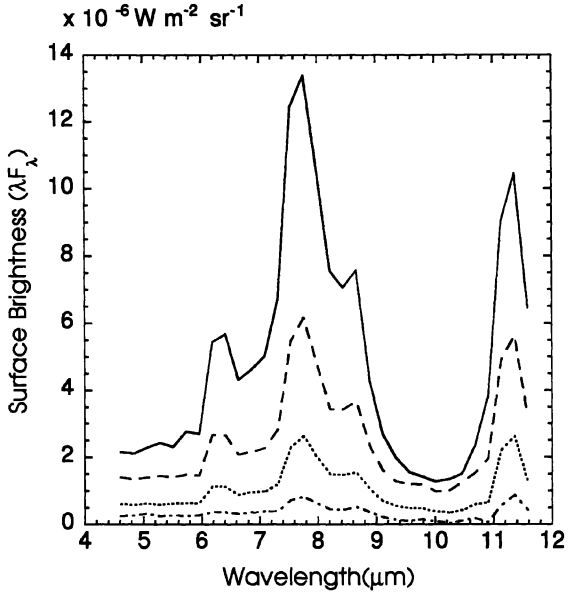

Fig. 1. Spectra of the diffuse emission around the galactic plane ($l \sim 50°$). The solid line indicates that for the region $44° \leq l \leq 44°40'$ and $-0°40' \leq b \leq 0°$, the dashed line for $1° \leq b < 2°$ ($50° \leq l \leq 53°$), the dotted line for $2° \leq b < 3°$ ($50° \leq l \leq 53°$), and the dot-dashed line for $3° \leq b \leq 5°$ and $51° \leq l \leq 54°$.

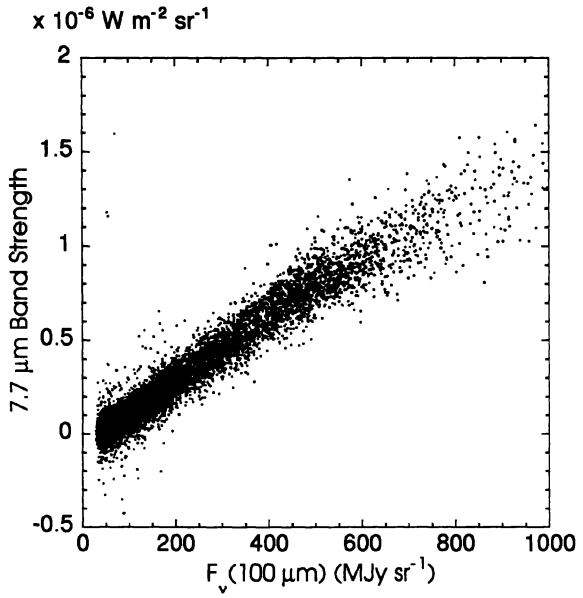

Fig. 3. The 7.7 μm band strength plotted against the ISSA 100 μm intensity.

8.22 μm, 8.22 and 9.12 μm, and 10.91 and 11.59 μm for the 6.2, 7.7, 8.6, and 11.3 μm bands, respectively. These continuum baselines are taken just sufficiently wide to extract the the band feature in order to minimize any possible effect of the remaining zodiacal emission. These fluxes may not completely include the entire emission associated with the bands, but do provide a good measure of the band strength for studying the spatial distributions. The present definition of the band strength is different from that in previous work (Cohen et al. 1986, 1989; Jourdain de Muizon et al. 1990; Zavagno et al. 1992).

Figures 2a–d (Plate 18) present color maps of the 6.2, 7.7, 8.6, and 11.3 μm band strengths. In figure 2a the IRAS Sky Survey Atlas (ISSA) 100 μm intensity contour, which traces the submicron dust-grain distribution (see below), is superposed (Wheelock et al. 1994). The slanted stripes of the colored region indicate the scanning direction and the observed area. The white spots in the stripes indicate the positions where the data are missing due either to a non-uniform scan coverage or to gaps in the flight data stream. The 3.3 μm band shows a similar distribution (Tanaka et al. 1996). The bright region at the center of the maps is the W51 complex, a very active star-forming region located in the Sagittarius arm (Bieging 1975). The spatial distributions of the four UIR bands are very similar to each other as well as to the 100 μm map.

In order to investigate the correlation between the UIR bands and the 100 μm flux more quantitatively, in figure 3 we plot the 7.7 μm band strength against the 100 μm intensity. In this figure, only the data points with the 100 μm intensity less than 1000 MJy sr^{-1} are plotted; also, the data in the W51 region are excluded in order to highlight the distribution of the diffuse emission. The correlation coefficient of the plot is 0.96. The other bands have similar correlations. The few points located far above the main concentration at small 100 μm intensities are due to poorly-corrected cosmic-ray hits, and should be ignored.

The 100 μm flux is understood to arise from the thermal emission of "classical" submicron size dust grains. Unless there is large variation in the temperature, the 100 μm flux should indicate the energy emitted by the dust grains and/or their column density. The investigation of the 160 μm emission obtained by the Far-Infrared Line Mapper (FILM) on board the IRTS suggests that the variation in the dust temperature is restricted to within a small range within the regions which we are addressing in this paper (Okumura et al. 1996). It is unlikely that there is large variation in the emission mechanism in the observed regions, except for the very active regions. Thus, the good correlation in figure 3 simply

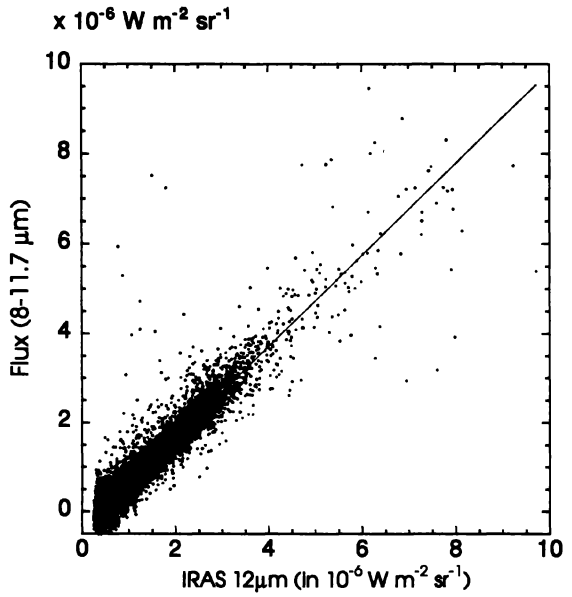

Fig. 4. Flux in the 8–11.7 μm of the MIRS spectrum plotted against the ISSA 12 μm intensity. The 12 μm intensity is converted into units of W m^{-2} sr^{-1} (see text). The solid line indicates the least-squares fit.

suggests that the UIR band carriers are well-mixed with the classical dust-grain population, or that the carriers exist in the submicron dust grains, themselves (Duley, Williams 1988).

Figure 4 is a plot of the flux falling in the spectral range 8–11.7 μm in the MIRS spectra against the ISSA 12 μm intensity. The ISSA intensity has been converted to units of W m^{-2} sr^{-1}, assuming a band width of 7 μm and νF_ν being constant. A good correlation is also seen. A least-squares fit, indicated by a solid line in the figure, has a slope of 1.0. If we take account of the 30% uncertainty in the absolute calibration and assume that the color correction in the ISSA intensity is not significant, approximately more than 70% of the ISSA 12 μm flux must come from the spectral range of 8–11.7 μm. As can be seen in figure 1, the emission from 8–11.7 μm is dominated by the wing of the 7.7 μm band, the 8.6 μm and 11.3 μm bands, and the plateau component. Thus, most of the ISSA 12 μm excess is due to those features associated with the UIR bands. Zavagno et al. (1992) indicated that mid-IR emission in most H II regions and reflection nebulae is dominated by the UIR band features, although there are large variations in the ratios of the band feature to the underlying continuum among the objects. The present results may indicate that the mid-IR interstellar diffuse emission is similar to that from those H II regions with the lowest continuum. Several points far above the main concentration at small 12 μm intensities are those from multiple observations of a strong point source IRC +10420; the observed scatter is caused by the large difference in the spatial resolution between the MIRS and IRAS data.

Ristorcelli et al. (1994) reported that the 6.2 μm band intensity ($\Delta\lambda I_\lambda$) detected by the AROME experiment is $(6.1 \pm 1.3) \times 10^{-7}$ W m^{-2} sr^{-1} in the region of $8° < l < 35°$ and $|b| < 1°$, where the 100 μm intensity (λI_λ) is 3.3×10^{-5} W m^{-2} sr^{-1}, giving a ratio of 0.018 ± 0.004. In the present observations, the ratio of the 6.2 μm band intensity to the 100 μm intensity $\Delta\lambda I_\lambda$(6.2 μm) /λI_λ(100 μm) is 0.012 ± 0.0002. Taking into account the uncertainty of the calibration and a possible underestimate of the band strength in the present study relative to the AROME experiment, this ratio is in agreement with Ristorcelli et al. (1994). This may imply that the emission efficiency and/or the population of the UIR-band carriers relative to the submicron dust grains do not vary much over a wide range throughout the galactic plane.

In summary, we have reported on the first results of the IRTS/MIRS spectra of the diffuse galactic emission in the range of 4.5–11.7 μm. They clearly demonstrate the presence of the UIR bands at 6.2, 7.7, 8.6, and 11.3 μm in the diffuse emission. Maps of the four UIR bands show a remarkable similarity to the 100 μm intensity distribution. This suggests that the UIR band carriers are well mixed with submicron-size dust grains in general interstellar space. A comparison of the intensity of the MIRS spectra in the range of 8–11.7 μm to the ISSA 12 μm intensity suggests that most of the ISSA 12 μm intensity comes from this spectral range, and particularly from the features associated with the UIR bands (the 7.7, 8.6, 11.3 μm bands, and the plateau component).

T.O. and T.T. would like to dedicate this short report to Akira Sakata, who passed away just right after the IRTS observation was completed without having a chance to see the first spectrum of the mid-IR diffuse emission. They are deeply indebted to his help during the development of the MIRS as well as to his continuous encouragement in the UIR band research. The authors thank Martin Cohen for providing the calibrated spectra of standard stars as well as the spectrum of Ceres taken at about the same time as the IRTS observations and IPAC for their help in the pointing reconstruction of the IRTS. They would also like to thank the SFU satellite project team for their efforts, without which the successful observations of the IRTS would not have been obtained. The ISSA data were obtained from NASA ADC. I.Y. is supported by the JSPS Research Fellowships for Young Scientists. He also thanks SRON-Groningen for their hospitality, where the last part of this work was

carried out. T.O. and T.T. are supported in part by a Grant-in-Aid from the Ministry of Education, Science, Sports and Culture in Japan. T.R. and L.Y. would like to acknowledge the support of the Astrophysics Grants Program of NASA. The IRTS is a joint mission between ISAS and NASA. The authors are grateful to all the members of the IRTS team for their help and pleasant discussions during the project.

References

Allamandola L.J., Bregman J.D., Sandford S.A., Tielens A.G.G.M., Witteborn, F.C., Wooden, D.H. 1989, ApJ 345, L59

Allamandola L.J., Tielens A.G.G.M., Barker J.R. 1985, ApJ 290, L25

Bieging J. 1975, in H II Regions and Related Topics, ed T.L. Wilson, D. Downes (Springer-Verlag, Heidelberg) p443

Borghesi A., Bussoletti E., Colangeli L. 1987, ApJ 314, 422

Boulanger F., Baud D., van Albada G.D. 1985, A&A 144, L9

Bregman J.D., Dinerstein H.L., Goebel J.H., Lester D.E., Witteborn F.C., Rank D.M. 1983, ApJ 274, 666

Cohen M., Allamandola L., Tielens A.G.G.M., Bregman J., Simpson J.P., Witteborn F.C., Wooden D., Rank D. 1986, ApJ 302, 737

Cohen M., Tielens A.G.G.M., Bregman J., Witteborn C., Rank D.M., Allamandola L.J., Wooden D.H., Jourdain de Muizon M. 1989, ApJ 341, 246

Cohen M., Witteborn F.C., Walker R.G., Bregman J.D., Wooden D.H. 1995, AJ 110, 275

Draine B.T., Anderson N. 1985, ApJ 292, 494

Duley W.W., Williams D.A. 1981, MNRAS 196, 269

Duley W.W., Williams D.A. 1988, MNRAS 231, 969

Giard M., Pajot F., Lamarre J.M., Serra G., Caux E. 1989, A&A 215, 92

Giard M., Pajot F., Lamarre J.M., Serra G., Caux E., Gispert R., Léger A., Rouan D. 1988, A&A 201, L1

Jourdain de Muizon M., d'Hendecourt L.B., Geballe T.R. 1990, A&A 227, 526

Léger A., Puget J.L. 1984, A&A 137, L5

Murakami H., Bock J., Freund M., Guo H., Hirao T., Lange A.E., Matsuhara H., Matsumoto T. et al. 1994, ApJ 428, 354

Murakami H., Freund M.M., Ganga K., Guo H., Hirao T., Hiromoto N., Kawada M., Lange A.E. et al. 1996, PASJ 48, L41

Okumura K., Shibai H., Okuda H., Nakagawa T., Makiuti S., Matsuhara H., Hiromoto N. 1996, PASJ submitted

Papoular R., Conard J., Guiliano M., Kister J., Mille G. 1989, A&A 217, 204

Puget J.L., Léger A., Boulanger F. 1985, A&A 142, L19

Ristorcelli I., Giard M., Mény C., Serra G., Lamarre J.M., Le Naour C., Létoin J., Pajot F. 1994, A&A 286, L23

Roellig T.L., Onaka T., McMahon T.J., Tanabé T. 1994, ApJ 428, 370

Sakata A., Wada S., Onaka T., Tokunaga A.T. 1987, ApJ 320, L63

Sakata A., Wada S., Tanabé T., Onaka T. 1984, ApJ 287, L51

Tanaka M., Kawada M., Matsumoto T., Murakami H., Matsuura S., Noda M. 1996, PASJ 48, L53

Wheelock S., Gautier T.N., Chillemi J., Kester D., McCallon H., Oken C., White J., Gregorich D. et al. 1994, IRAS Sky Survey Atlas Explanatory Supplement, JPL Publication 94-11

Yamamura I., Onaka T., Tanabé T., Roellig T.L., Yuen L. 1996, PASJ 48, L65

Zavagno A., Cox P., Baluteau J.-P. 1992, A&A 259, 241

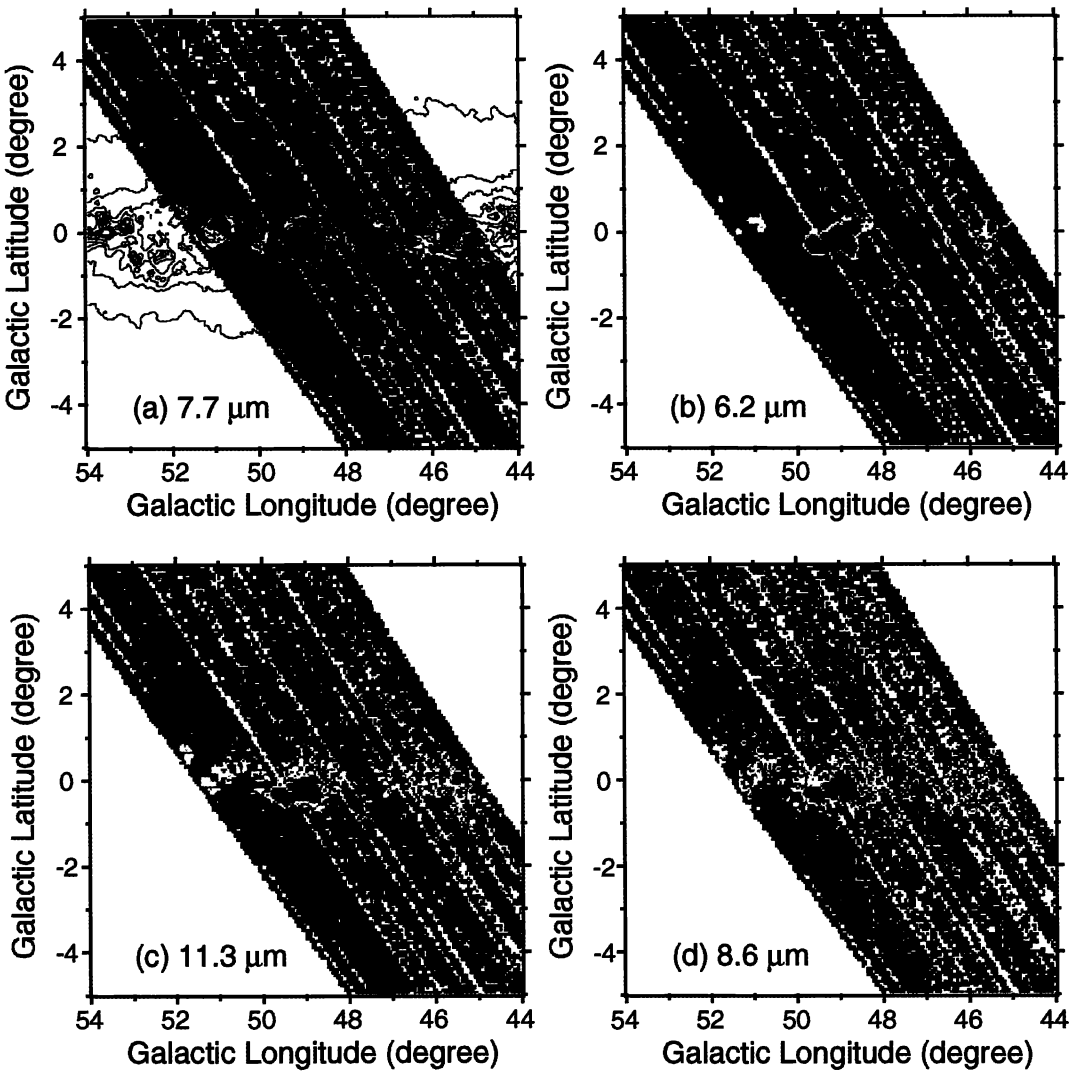

Fig. 2. Maps of the UIR bands (see text for the definition of the band strengths). a) The 7.7 μm band is shown in color. The contour is the ISSA 100 μm intensity with contours ranging from 100 MJy sr^{-1} to 1000 MJy sr^{-1} with a step of 100 MJy sr^{-1}. The contours larger than 1000 MJy sr^{-1} are omitted for clarity. b) The 6.2 μm band map. c) The 11.3 μm band map. d) The 8.6 μm band map.